Wrinkling of the membrane with square rigid elements

2016 EPL 116 24005

(http://iopscience.iop.org/0295-5075/116/2/24005)

A Letters Journal Exploring the Frontiers of Physics

October 2016

EPL, **116** (2016) 24005 www.epljournal.org
doi: 10.1209/0295-5075/116/24005

Wrinkling of the membrane with square rigid elements

Dong Yan[1], Dongzhen Huangfu[2], Kai Zhang[1,3(a)] and Gengkai Hu[1]

[1] *School of Aerospace Engineering, Beijing Institute of Technology - Beijing 100081, China*
[2] *School of Mechatronical Engineering, Beijing Institute of Technology - Beijing 100081, China*
[3] *Key Laboratory of Autonomous Navigation and Control for Deep Space Exploration, Ministry of Industry and Information Technology, Beijing Institute of Technology - Beijing 100081, China*

received 21 September 2016; accepted in final form 15 November 2016
published online 30 November 2016

PACS 46.32.+x – Static buckling and instability
PACS 46.70.De – Beams, plates, and shells

Abstract – Heterogeneous membrane with rigid elements has been extensively applied in flexible electronic systems and in aerospace structures. Here, we study the surface wrinkling of such heterogeneous membrane. Experiment, theoretical analysis and numerical simulation are performed to quantify the effect of rigid elements on the wrinkle pattern of the membrane. The characteristics of wrinkles related to the positions of rigid elements and stretching strain are investigated and the underlying mechanism is revealed. It is found that wrinkle patterns can be tailored by varying the positions of the rigid elements to achieve desired functions. Our results can provide insightful ideas to understand the wrinkling phenomenon of heterogeneous membranes and create novel wrinkle patterns in a controllable way.

Introduction. – Wrinkling induced by instability of thin membranes is commonly encountered in micro/nanoengineering [1–3], biomedical engineering [4–7] and aerospace engineering [8–12]. Different wrinkle patterns in membrane systems can achieve desired functions [1–6,13]. For example, ordered micro/nanostructures formed by surface wrinkling on a thin membrane offer considerable interests and numerous applications as stretchable electronics [3]. On the other hand, surface wrinkles are sometimes needed to be suppressed, such as membrane antenna in aerospace engineering, which demands very smooth surfaces with few wrinkles [8–12]. The study of controllable wrinkle patterns of soft material systems provides both fundamental insights and practical guidance for engineering design. Though the membranes used in practice are usually heterogeneous [3,12,14–18], such as the flexible electronics with rigid circuits [3,16] or the aerospace membrane antenna with electronic elements [12], most of the efforts focus on the wrinkling of uniform membranes [7–11,19–22], and the influence of heterogeneous materials on the wrinkle pattern has not received much attentions [12,14–17,23–29]. Here we focus on a two-end clamped membrane with square rigid elements under stretching to study the wrinkling of the heterogeneous membrane. We reveal the underlying mechanism of wrinkling and analyze the wrinkle pattern by varying the positions of rigid elements in both experiment and numerical simulation. The wrinkle pattern of a two-end clamped membrane is effectively controlled by designing the arrangement of rigid elements. Our results are helpful for the design of aerospace membrane structure, and also useful in micro/nanoengineering and biomedical engineering.

Experiment and observations. – We consider a polyimide membrane with a size of $100 \times 40 \times 0.025\,\mathrm{mm}^3$ (length $2L \times$ width $2C \times$ thickness t). The elastic modulus of the uniform polyimide membrane is measured to be 2.88 ± 0.11 GPa by tensile testing and the Poisson ratio is assumed to be 0.31 according to ref. [9]. To study the effect of rigid elements on the wrinkle pattern of the membrane in both horizontal and vertical directions, four square rigid elements with side lengths of 4 mm and thicknesses of 0.5 mm are fixed on the membrane symmetrically by using cyanoacrylate adhesive, as shown in fig. 1. The square rigid element is made of aluminum, whose elastic modulus is about 69 GPa and much larger than that of the membrane. By varying the horizontal distance ($2x_0$) and the vertical distance ($2y_0$) between the centers of two rigid elements, six different kinds of heterogeneous membranes are made. Then all of the rectangular membranes with four rigid elements, whose two ends are clamped,

(a) E-mail: zhangkai@bit.edu.cn (corresponding author)

are subjected to a uniaxial stretching by a tensile machine (MTS, Eden Prairie, MN, USA). The resolutions of force and displacement of the tensile machine are 0.01 N and 0.001 mm, respectively, with maximum force 250 N and maximum displacement 600 mm. The applied tensile strain ε_x is 6% with a strain rate of 0.6% min^{-1}. Two lamps are placed in front of the membrane with angles of about 45° and −45°, respectively, to the normal of the membrane. A digital camera perpendicular to the membrane is used to capture the images of the membrane during stretching as shown in fig. 1. According to the previous works about the wrinkling of a stretched uniform membrane with clamped ends [7,15,19,20], the sine-shape wrinkles are parallel to the loading direction in the central region of the membrane due to the Poisson effect. In comparison, the heterogeneous membranes under stretching display several different kinds of wrinkle patterns, shown in fig. 1. When the four rigid elements are located together in the central region of the membrane in fig. 1(a), the horizontal regions near the rigid elements remain flat but wrinkle far from the rigid elements along the horizontal center line, with smaller wavelength compared with that of a uniform membrane. Furthermore, the rigid elements trigger the wrinkling of vertical local regions around the rigid elements. As a result, two different sets of wrinkles appear on one membrane. Subsequently, when the four rigid elements are separated by increasing the distance between them, two contrary wrinkling phenomena are triggered with varied x_0/L and unchanged $y_0/C = 0.40$. When $x_0/L = 0.10$ in fig. 1(b), no wrinkle is observed between two horizontal rigid elements, whereas a new wrinkle pattern is exhibited in the region between rigid element and clamped end. As for the heterogeneous membranes with increasing $x_0/L = 0.40$ or 0.80 (figs. 1(c) and (d)), wrinkles appear in the region between two horizontal rigid elements, disappearing in the region between rigid element and clamped end. As a special case, when the rigid elements are located far away from each other ($x_0/L = 0.80$) as shown in fig. 1(d), a wrinkle pattern similar to that of the uniform membrane can be observed, indicating that the rigid elements have little effect on the wrinkling of the membrane. Finally, when y_0/C is increased to be 0.80, the central region of membrane can almost remain flat ($x_0/L = 0.80$ in fig. 1(e)), or be wrinkled seriously ($x_0/L = 0.10$ in fig. 1(f)). It is noted that wrinkling in the vertical local regions around each rigid element almost arises for all the cases in fig. 1. The wrinkle patterns in fig. 1 are entirely different from that of the uniform membrane, demonstrating that the rigid elements play an important role in the wrinkling of membrane.

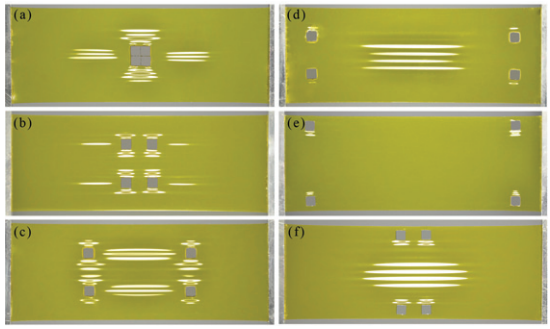

Fig. 1: (Colour online) Wrinkle patterns of the two-end clamped membrane with four rigid elements at different positions under stretching. The applied stretching strain ε_x is 6%. (a) $x_0/L = 0.04$, $y_0/C = 0.10$, (b) $x_0/L = 0.10$, $y_0/C = 0.40$, (c) $x_0/L = 0.40$, $y_0/C = 0.40$, (d) $x_0/L = 0.80$, $y_0/C = 0.40$, (e) $x_0/L = 0.80$, $y_0/C = 0.80$ and (f) $x_0/L = 0.10$, $y_0/C = 0.80$.

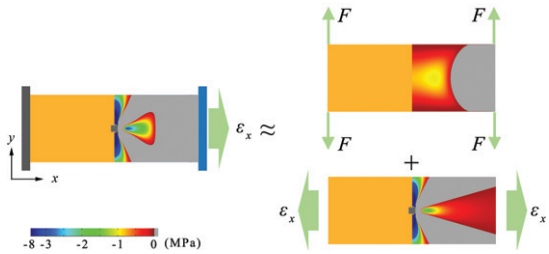

Fig. 2: (Colour online) Schematic and stress fields (σ_y) of the approximate mechanical model for a two-end clamped membrane with a square rigid element under stretching. The stretching strain ε_x is 6%.

Results and discussion. –

Effect of the square rigid element on stress distribution. As a prerequisite for wrinkling, development of compressive stress can determine the wrinkle pattern on the membrane. Here we start from the normal stress in the transverse direction (σ_y) of a two-end clamped membrane with only one rigid element at the center to explain the effect of rigid element on stress distribution. For the two-end clamped membrane with one rigid element under stretching, the stress field is proposed to be approximately described by the superposition of two parts: the membrane under uniform tension and under four concentrated forces at the corners of the membrane [15]. We further neglect the rigid element in the model of the membrane under four concentrated forces as shown in fig. 2, and the analytical stress solution of a uniform membrane under four concentrated forces is used. The corresponding stress field can be expressed by using Fourier series as [15]

$$\sigma_{x1} = \frac{2F}{L}\sum_{m=1}^{\infty}\left[\left(A - \frac{B}{m_\lambda}\right)\cosh\left(m_\lambda y_r\right) - By_r\sinh\left(m_\lambda y_r\right)\right]\cos\left(\frac{m_\lambda}{\lambda}x_r\right),$$

$$\sigma_{y1} = \frac{F}{L} - \frac{2F}{L}\sum_{m=1}^{\infty}\left[\left(A + \frac{B}{m_\lambda}\right)\cosh\left(m_\lambda y_r\right) - By_r\sinh\left(m_\lambda y_r\right)\right]\cos\left(\frac{m_\lambda}{\lambda}x_r\right),$$

$$\begin{aligned}\tau_{xy1} &= \frac{2F}{L}\sum_{m=1}^{\infty}\Big[A\sinh\left(m_\lambda y_r\right)\\ &\quad - By_r\cosh\left(m_\lambda y_r\right)\Big]\sin\left(\frac{m_\lambda}{\lambda}x_r\right),\\ A &= (-1)^m\frac{-m_\lambda\cosh m_\lambda}{\cosh m_\lambda\sinh m_\lambda + m_\lambda},\\ B &= (-1)^m\frac{-m_\lambda\sinh m_\lambda}{\cosh m_\lambda\sinh m_\lambda + m_\lambda},\end{aligned} \tag{1}$$

where $x_r = x/L$ and $y_r = y/C$ are the coordinates along the length and width directions, respectively, with the origin at the center of the membrane. $\lambda = C/L$ is the width-length ratio and $m_\lambda = m\pi\lambda$. The concentrated force F is $0.38\nu\varepsilon_x EC$, where 0.38 is an equivalent factor between the concentrated force and the nonuniform distributed shear force induced by the clamped end [15]. E and ν are the elastic modulus and Poisson ratio of the membrane, respectively. Taking σ_{y1} into account, according to eq. (1), there is large tensile stress distributing near the clamped ends and very small compressive stress in the central region far from the clamped ends due to the Poisson effect (fig. 2).

The stress of a membrane with a square rigid element under uniform tension can be approximated to that of an infinite membrane with a square rigid element under uniform tension, which can be solved in curvilinear coordinate [30,31] based on complex function as

$$\begin{aligned}&\sigma_{y2} + \sigma_{x2} = 4\mathrm{Re}\Phi\left(\xi\right),\\ &\sigma_{y2} - \sigma_{x2} + 2\mathrm{i}\tau_{xy2} = 2\left[\frac{\overline{w\left(\xi\right)}}{w'\left(\xi\right)}\Phi'\left(\xi\right) + \Psi(\xi)\right],\end{aligned} \tag{2}$$

where

$$\begin{aligned}w(\xi) &= x + \mathrm{i}y = \frac{3}{5}a\left(\frac{1}{\xi} - \frac{1}{6}\xi^3\right),\\ \xi &= \rho\mathrm{e}^{\mathrm{i}\theta}\quad(0 < \rho \le 1,\ 0 \le \theta < 2\pi),\\ \Phi\left(\xi\right) &= \frac{E\varepsilon_x}{2+\xi^4}\left[\frac{1}{2} + \frac{6\left(1+\nu\right)}{17-7\nu}\xi^2 + \frac{1+\nu}{4\left(3-\nu\right)}\xi^4\right],\\ \Psi(\xi) &= -\frac{E\varepsilon_x}{2+\xi^4}\left[1 + \frac{\left(1-\nu\right)\left(35-13\nu\right)}{12\left(1+\nu\right)\left(3-\nu\right)}\xi^2\right.\\ &\quad - \frac{13\left(1+\nu\right)}{17-7\nu}\frac{6-\xi^4}{\left(2+\xi^4\right)^2}\xi^4\\ &\quad \left. + \frac{13\left(1-\nu\right)}{12\left(3-\nu\right)}\frac{10+\xi^4}{\left(2+\xi^4\right)^2}\xi^6\right].\end{aligned} \tag{3}$$

a is the side length of the square rigid element. The corresponding stress field σ_{y2} is shown in fig. 2. The introduced rigid element, which is similar to a local clamped end, prevents the deformation of the stretched membrane, bringing an inhomogeneous stress field and resulting in the redistribution of stress in the membrane. As a consequence, the stress σ_{y2} is tensile near the rigid element but compressive far from the rigid element along the horizontal center line. On the other hand, compressive stress is generated in vertical regions around the rigid element, extending up to the free edges of the membrane.

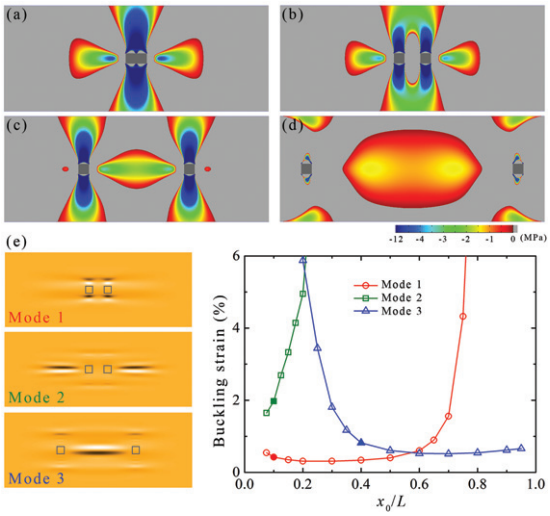

Fig. 3: (Colour online) Stress fields (σ_y) of the two-end clamped membrane with two rigid elements at different horizontal positions under stretching: (a) $x_0/L = 0.04$, (b) $x_0/L = 0.10$, (c) $x_0/L = 0.40$ and (d) $x_0/L = 0.80$. The stretching strain ε_x is 6%. (e) Eigen buckling modes and corresponding buckling strains *vs.* the horizontal position of rigid elements by numerical eigenvalue buckling analysis.

Then the stress field σ_y in a two-end clamped membrane with a rigid element under stretching is described by the superposition of σ_{y1} and σ_{y2}. Both tensile and compressive stresses in the regions around rigid elements are mainly caused by the mismatched elastic moduli of rigid element and membrane, whereas the relative small compressive stress induced by the clamped ends can be completely ignored when the membrane is long enough. The analytical stress field has a good agreement with the numerical result by FEM [31].

Effect of the distances between square rigid elements on the wrinkle pattern. Now we consider a two-end clamped membrane with two square rigid elements to study the effect of horizontal distance on the wrinkle pattern by theoretical and numerical analysis. When two rigid elements are arranged on the two-end clamped membrane, the stress field in the membrane can be described approximately by superposing the stress field of a uniform membrane and stress fields caused by each rigid element in fig. 2. The stress fields of the membrane with two rigid elements at different horizontal positions are shown in figs. 3(a)–(d), which have a good agreement with the FEM results [31]. When the rigid elements are located far from the clamped ends, the rigid elements play an important role to determine the final stress distribution between the rigid elements, and stress induced by the clamped ends

can be neglected. For example, separating the two rigid elements with a small distance $x_0/L = 0.10$ can eventually generate an obvious local tensile region between the two rigid elements (fig. 3(b)). However, as x_0/L increases, *e.g.*, $x_0/L = 0.40$ shown in fig. 3(c), compressive stress induced by the rigid elements appears in the region between the two horizontal rigid elements, resulting in local wrinkles between the two rigid elements. On the contrary, when the rigid elements along the horizontal center line are separated sufficiently and located near the clamped ends, the stress field is mainly determined by clamped ends while the effect of the rigid elements is weak, as shown in fig. 3(d) ($x_0/L = 0.80$). In addition, the coupling effect between rigid element and clamped end is determined by the position of the rigid element. In the horizontal region between rigid element and clamped end in fig. 3(c), the compressive stress induced by the rigid element is neutralized by the tensile stress induced by the clamped end. Thus, the wrinkles in this region gradually disappear.

As a result, the variation on the distribution of compressive stress decides the different eigen buckling modes of the membrane. Three buckling modes distinguished by the buckled region are shown in fig. 3(e). In Mode 1, wrinkles occur in the vertical regions of the rigid elements. In Mode 2 and Mode 3, wrinkles are triggered in horizontal regions between rigid element and clamped end and between two rigid elements, respectively. When the distance x_0/L is small, the membrane first deforms into the lowest buckling mode (Mode 1) and then Mode 2, comparing with an infinite buckling strain of Mode 3 due to the tensile state between the two rigid elements. With increasing distance x_0/L, the stress between the two rigid elements gradually transforms from tensile to compressive, decreasing the buckling strain of Mode 3. A turnover of the lowest buckling mode occurs up to a critical point $x_0/L = 0.57$: The lowest buckling mode transforms from Mode 1 to Mode 3. Subsequently, the buckling strains of both Mode 1 and Mode 2 remarkably increase with the raising distance as a result of the effect of the clamped end, leading to eventual disappearance of both Mode 1 and Mode 2. The results are consistent with the experimental observations in fig. 1.

We characterize the wrinkles between two horizontal rigid elements in postbuckling analysis by FEM [32,33]. The normalized wrinkle wavelength (λ_x/L) related to the normalized horizontal distance (x_0/L) and stretching strain (ε_x) is shown in fig. 4(a). λ_x/L increases with x_0/L but decreases with ε_x. By fitting the data of normalized wavelength as a function of normalized horizontal distance and stretching strain, we find the normalized wavelength complies with the scaling law (fig. 4(a)) as

$$\frac{\lambda_x}{L} \sim \left(\frac{x_0}{L}\right)^{\frac{1}{2}} \varepsilon_x^{-\frac{1}{4}}. \tag{4}$$

The scaling relationship $\lambda_x \sim \varepsilon_x^{-1/4}$ is the same as that for a uniform membrane [7,19] except for the new introduced

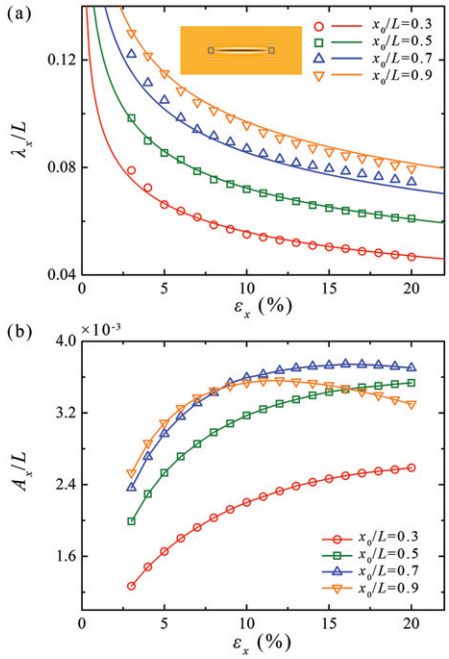

Fig. 4: (Colour online) Normalized wrinkle wavelength λ_x/L against stretching strain ε_x for various normalized horizontal distance x_0/L. Symbols represent the calculated results by FEM and lines are the scaling law $\lambda_x/L = 0.0575(x_0/L)^{1/2}\varepsilon_x^{-1/4}$. (b) Normalized wrinkle amplitude A_x/L against stretching strain ε_x for various normalized horizontal distance x_0/L. Symbols connected by lines are calculated by FEM.

term $x_0^{1/2}$, which represents the effect of heterogeneity of the membrane with rigid elements. Hence, the membrane with rigid elements possesses the ability to tune the wavelength of wrinkles by designing the distance between two horizontal rigid elements. In eq. (4), we only consider the dependence of wavelength on the horizontal distance between rigid elements and tensile strain for a two-end clamped membrane under stretching. The wavelength also relates to the sizes of rigid element and membrane, which would be necessary for further studies. We quantify the normalized wrinkle amplitude (A_x/L) as shown in fig. 4(b). For normalized horizontal distance x_0/L between 0.3 and 0.7, A_x/L increases with stretching strain, and a larger x_0/L results in a larger A_x/L. However, when the horizontal distance is too large, such as $x_0/L = 0.9$ in fig. 4(b), A_x/L will first increase and then decrease, which is similar to the uniform membrane [20].

The effect of the vertical distance y_0/C on the stress field is also taken into account and the stress fields of the membrane with two rigid elements at different vertical positions are shown in figs. 5(a)–(d), which also have a good agreement with the FEM results [31]. The two rigid elements are located in the vertical center line far from the clamped ends, hence only small compressive stress is induced by the clamped ends in this region. Thus, the stress distribution near the rigid elements is mainly determined by the rigid elements. Moving the rigid elements towards

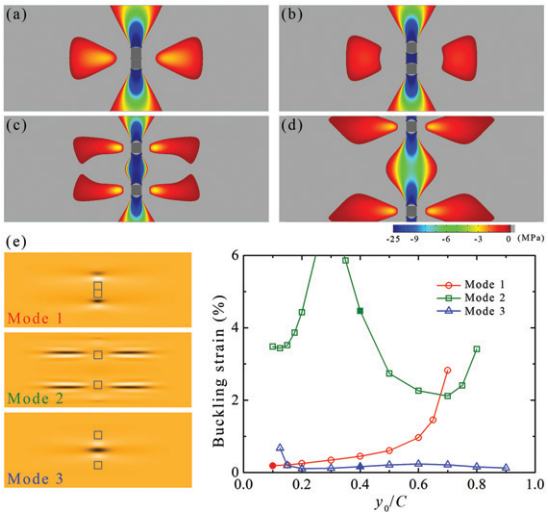

Fig. 5: (Colour online) Stress fields (σ_y) of the two-end clamped membrane with two rigid elements at different vertical positions under stretching: (a) $y_0/C = 0.10$, (b) $y_0/C = 0.20$, (c) $y_0/C = 0.40$ and (d) $y_0/C = 0.80$. The stretching strain ε_x is 6%. (e) Eigen buckling modes and corresponding buckling strains *vs.* the vertical position of rigid elements by numerical eigenvalue buckling analysis.

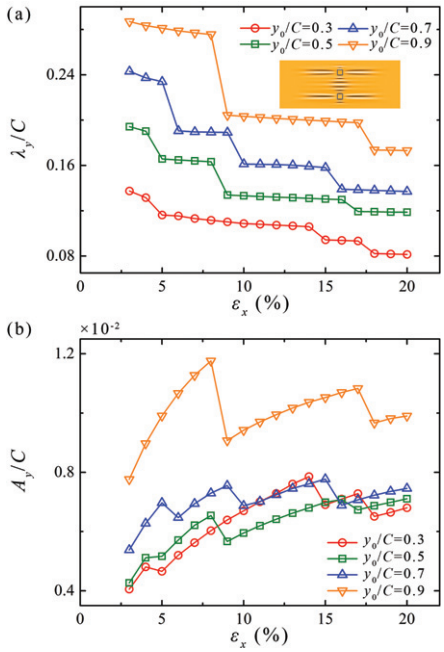

Fig. 6: (Colour online) Normalized wrinkle wavelength λ_y/C (a) and amplitude A_y/C (b) against stretching strain ε_x for various normalized vertical distance y_0/C. Symbols connected by lines are calculated by FEM.

the upper and lower free edges with increasing vertical distance y_0/C from 0.10 (fig. 5(a)) to 0.20 (fig. 5(b)), 0.40 (fig. 5(c)) and 0.80 (fig. 5(d)), the vertical regions of each rigid element are always under compression, and the compressive region between the rigid elements gradually expands. Thus, the compressive stress can trigger the local wrinkling around the rigid elements and between the vertical rigid elements (fig. 1), corresponding to Mode 1 and Mode 3 (fig. 5(e)), respectively. More importantly, a field of tensile stress, generated by the rigid elements in the oblique direction, relaxes the compressive stress induced by the clamped ends when the rigid elements are fixed near the two free edges of the membrane. Hence, when the rigid elements are located near the corners of the membrane as shown in fig. 1(e), the tensile stress in the oblique direction of the rigid elements eliminates the wrinkles on the whole membrane.

The wavelength and amplitude of wrinkles between two vertical rigid elements are also quantified in postbuckling analysis by FEM. The normalized wrinkle wavelength (λ_y/C) and amplitude (A_y/C) related to the normalized vertical distance (y_0/C) and stretching strain (ε_x) are shown in figs. 6(a) and (b), respectively. λ_y/C decreases and A_y/C increases with stretching strain accompanied by some sudden drops, where more wrinkles are triggered as a result of minimizing the potential energy of the system. A larger y_0/C results in a larger λ_y/C. A_y/C also increases with rising y_0/C, but the increase is not obvious when y_0/C is small.

Now we go back to the wrinkle pattern of the membrane with four rigid elements at different positions. Besides the wrinkle patterns observed in experiment (fig. 1), a phase diagram of wrinkle pattern of the membrane with four rigid elements related to the positions of rigid elements is shown in fig. 7 by numerical postbuckling analysis, showing the ability to control wrinkle patterns by changing the distances between rigid elements.

Wrinkle pattern of a two-end clamped membrane with periodic arranged square rigid elements. When rigid elements are arranged on the membrane in a periodic pattern and then under uniaxial stretching, different wrinkle patterns are created by designing the positions of rigid elements as shown in fig. 8. Surface accuracy of thin membrane is one of the key requirements for membrane antenna in aerospace engineering. Suitable horizontal distance between rigid elements can generate a tensile field and further suppress the local wrinkles in the horizontal regions (fig. 8(a)). The tensile region near the rigid element can be estimated by solving $\sigma_{y2}|_{y=0} = 0$. Then an approximate solution for the critical distance between the centers of two horizontal rigid elements ($d_{\rm cr}$) is obtained as

$$d_{\rm cr} = 2\left(\frac{7}{3}\nu + \frac{2}{3}\right)a, \tag{5}$$

where ν ($\nu \geq 0.2$) and a are the Poisson ratio of the membrane and side length of the rigid element, respectively. The critical distance is important for designing the distribution of periodic rigid elements on membrane. When the distance between the centers of two horizontal rigid elements is smaller than $d_{\rm cr}$, compressive stress in the region

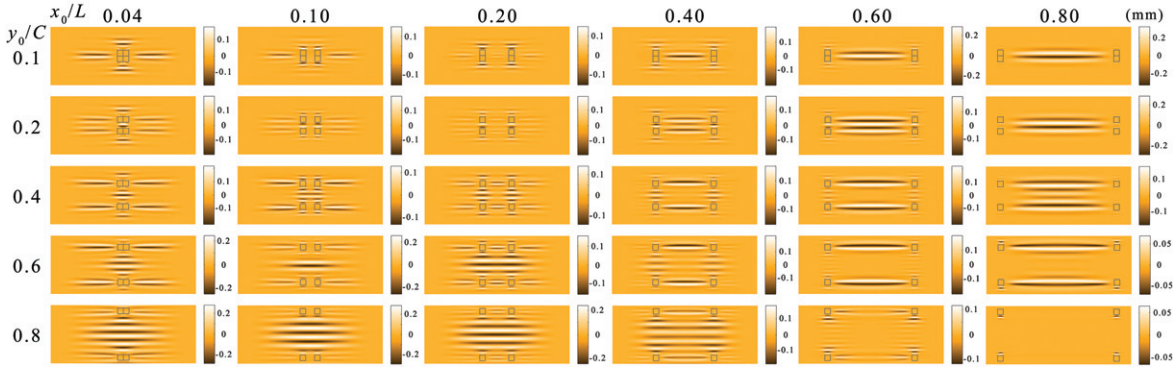

Fig. 7: (Colour online) Wrinkle patterns of the two-end clamped membrane with four rigid elements related to the positions of rigid elements by numerical postbuckling analysis. The stretching strain ε_x is 6%.

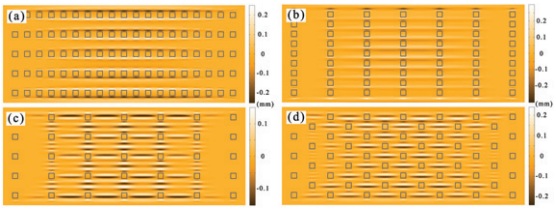

Fig. 8: (Colour online) Wrinkle patterns of the membranes with periodic rigid elements with different horizontal (d_x) and vertical (d_y) distances at 3% stretching strain: (a) $d_x = 10\,\text{mm}$, $d_y = 16\,\text{mm}$, (b) $d_x = 30\,\text{mm}$, $d_y = 8\,\text{mm}$ and (c) $d_x = 30\,\text{mm}$, $d_y = 16\,\text{mm}$. (d) $d_x = 30\,\text{mm}$, $d_y = 16\,\text{mm}$ in hexagonal pattern. The size of membrane is $200 \times 80 \times 0.025\,\text{mm}^3$ (length × width × thickness), and the side length of the rigid element is 4 mm.

between them will be weakened, which even flattens the membrane. As an approximate model, eq. (5) may be used to qualitatively understand the wrinkling between horizontal rigid elements as well as the dependence on the Poisson ratio of the membrane and side length of the rigid element. It is noted that, the critical distance in eq. (5) is calculated from eqs. (2), (3) which is the stress induced by a square rigid element in a two-end clamped membrane under stretching. For the rigid element with other shapes in a two-end clamped membrane, the critical distance can be obtained by the same method. In addition, the wrinkles can also be suppressed due to the tensile stress in the oblique direction caused by adjacent rigid elements (fig. 8(b)), compared with the wrinkle pattern in fig. 8(c).

On the other hand, regardless of the position of the rigid element, local wrinkles in the region between two vertical rigid elements are always not avoided due to the compressive stress induced by individual rigid element. As a consequence, a complex wrinkle pattern with two different sets of wrinkles on one membrane system can be created (fig. 8(c)). In comparison, a periodic wrinkle pattern with only one set of wrinkles in all wrinkled regions can be tailored on the membrane by arranging the rigid elements in a hexagonal lattice (fig. 8(d)).

In our previous work, it is reported that punching holes can also achieve desired wrinkle patterns in the membrane or suppress the wrinkles spanning the whole membrane [15]. Comparing with holes, the rigid elements exhibit a different effect on the modification of the stress field in the membrane. For example, there is a tensile region near the rigid element and a compressive region far from the rigid element along the horizontal center line of the membrane. But the trend is reversed for the stress caused by a hole, *i.e.*, a remarkable compressive region near the hole and a tensile region relatively far from the hole. In addition, an individual rigid element results in tensile regions in the oblique direction, while compressive regions in the oblique direction of a hole can be generated to trigger high-order local wrinkles [15,27]. Thus, wrinkles decorated on the whole membrane can be eliminated by locating the rigid elements near the upper and lower edges (fig. 1(e)) or by punching holes along the horizontal center line of the stretched membrane near the clamped ends [15].

Conclusions. – We have investigated the wrinkle patterns on a two-end clamped rectangular membrane with square rigid elements under stretching by changing the positions of the rigid elements. The rigid elements trigger an inhomogeneous stress field and the distribution of stress in the membrane is determined by the competition between the stress induced by clamped ends and the stress induced by rigid elements. When the rigid elements are located far from the clamped ends, the stress field is mainly induced by the rigid elements, while the effect of the rigid elements is weak when the rigid elements are located near the clamped ends. The rigid elements can make the two-end clamped rectangular membrane display a desired wrinkle pattern or even a suppression of wrinkles under stretching which may be applied in various disciplines, such as membrane manufacturing, flexible electronics and aerospace engineering.

* * *

Support from NSFC (Grant Nos. 11202025, 11290153, 11472044 and 11672037) is acknowledged.

REFERENCES

[1] Lee W. K., Engel C. J., Huntington M. D., Hu J. and Odom T. W., *Nano Lett.*, **15** (2015) 5624.

[2] Pereira V. M., Castro Neto A. H., Liang H. Y. and Mahadevan L., *Phys. Rev. Lett.*, **105** (2010) 156603.

[3] Rogers J. A., Someya T. and Huang Y., *Science*, **327** (2010) 1603.

[4] Bae H. J., Bae S., Park C., Han S., Kim J., Kim L. N., Kim K., Song S. H., Park W. and Kwon S., *Adv. Mater.*, **27** (2015) 2083.

[5] Efimenko K., Rackaitis M., Manias E., Vaziri A., Mahadevan L. and Genzer J., *Nat. Mater.*, **4** (2005) 293.

[6] Li B., Cao Y. P., Feng X. Q. and Gao H., *Soft Matter*, **8** (2012) 5728.

[7] Cerda E. and Mahadevan L., *Phys. Rev. Lett.*, **90** (2003) 074302.

[8] Jenkins C. H., Haugen F. and Spicher W. H., *Exp. Mech.*, **38** (1998) 147.

[9] Wong Y. W. and Pellegrino S., *J. Mech. Mater. Struct.*, **1** (2006) 1.

[10] Wang C. G., Du X. W., Tan H. F. and He X. D., *Int. J. Solids Struct.*, **46** (2009) 1516.

[11] Lecieux Y. and Bouzidi R., *Int. J. Solids Struct.*, **47** (2010) 2459.

[12] Fleurent-Wilson E., Pollock T. E., Su W. J., Warrier D. and Salehian A., *J. Intell. Mater. Syst. Struct.*, **25** (2014) 1978.

[13] Rudykh S. and Boyce M. C., *Phys. Rev. Lett.*, **112** (2014) 034301.

[14] Yan D., Zhang K. and Hu G., *Soft Matter*, **12** (2016) 3937.

[15] Yan D., Zhang K., Peng F. and Hu G., *Appl. Phys. Lett.*, **105** (2014) 071905.

[16] Takei A., Brau F., Roman B. and Bico J., *EPL*, **96** (2011) 64001.

[17] Muller P. and Kierfeld J., *Phys. Rev. Lett.*, **112** (2014) 094303.

[18] Zhang K., Duan H., Karihaloo B. L. and Wang J., *Proc. Natl. Acad. Sci. U.S.A.*, **107** (2010) 9502.

[19] Cerda E., Ravi-Chandar K. and Mahadevan L., *Nature*, **419** (2002) 579.

[20] Nayyar V., Ravi-Chandar K. and Huang R., *Int. J. Solids Struct.*, **51** (2014) 1847.

[21] Huang Z. Y., Hong W. and Suo Z., *J. Mech. Phys. Solids*, **53** (2005) 2101.

[22] Wang X. F., Yang Q. S. and Law S. S., *Int. J. Solids Struct.*, **51** (2014) 3532.

[23] Bowden N., Brittain S., Evans A. G., Hutchinson J. W. and Whitesides G. M., *Nature*, **393** (1998) 146.

[24] Huck W. T. S., Bowden N., Onck P., Pardoen T., Hutchinson J. W. and Whitesides G. M., *Langmuir*, **16** (2000) 3497.

[25] Croll B. and Crosby A. J., *Macromolecules*, **45** (2012) 4001.

[26] Ebata Y. and Crosby A. J., *Soft Matter*, **10** (2014) 1963.

[27] Flores-Johnson E. A., Rupert T. J., Hemker K. J., Gianola D. S. and Gan Y., *Extreme Mech. Lett.*, **4** (2015) 175.

[28] Lee J. H., Ro H. W., Huang R., Lemaillet P., Germer T. A., Soles C. L. and Stafford C. M., *Nano Lett.*, **12** (2012) 5995.

[29] Guo C. F., Nayyar V., Zhang Z., Chen Y., Miao J., Huang R. and Liu Q., *Adv. Mater.*, **24** (2012) 3010.

[30] Timoshenko S. P. and Goodier J. N., *Theory of Elasticity* (McGraw-Hill Book Company, Tokyo) 1970, p. 179.

[31] See supplemental material at, `https://drive.google.com/open?id=0B0hKoihXAXb6YkxKSlQ1VEJURTQ`.

[32] Tessler A., Sleight D. W. and Wang J. T., *J. Spacecr. Rockets*, **42** (2005) 287.

[33] Wong Y. W. and Pellegrino S., *J. Mech. Mater. Struct.*, **1** (2006) 61.